Steel and Composite Structures, *Vol. 33, No. 4* (*2019*) *583-594*
DOI: https://doi.org/10.12989/scs.2019.33.4.583

Prediction of ultimate load capacity of concrete-filled steel tube columns using multivariate adaptive regression splines (MARS)

Cigdem Avci-Karatas*

Department of Transportation Engineering, *Faculty of Engineering*, *Yalova University*, *Yalova*, *77200*, *Turkey*

(*Received June 5, 2019, Revised September 9, 2019, Accepted September 26, 2019*)

Abstract. In the areas highly exposed to earthquakes, concrete-filled steel tube columns (CFSTCs) are known to provide superior structural aspects such as (i) high strength for good seismic performance (ii) high ductility (iii) enhanced energy absorption (iv) confining pressure to concrete, (v) high section modulus, etc. Numerous studies were reported on behavior of CFSTCs under axial compression loadings. This paper presents an analytical model to predict ultimate load capacity of CFSTCs with circular sections under axial load by using multivariate adaptive regression splines (MARS). MARS is a nonlinear and non-parametric regression methodology. After careful study of literature, 150 comprehensive experimental data presented in the previous studies were examined to prepare a data set and the dependent variables such as geometrical and mechanical properties of circular CFST system have been identified. Basically, MARS model establishes a relation between predictors and dependent variables. Separate regression lines can be formed through the concept of divide and conquers strategy. About 70% of the consolidated data has been used for development of model and the rest of the data has been used for validation of the model. Proper care has been taken such that the input data consists of all ranges of variables. From the studies, it is noted that the predicted ultimate axial load capacity of CFSTCs is found to match with the corresponding experimental observations of literature.

Keywords: concrete-filled steel tube column (CFSTC); concrete; steel; modeling; ultimate axial load capacity; multivariate adaptive regression splines (MARS); composite structures; statistical modeling technique; nonlinear regression model

1. Introduction

Concrete-filled steel tubes (CFSTs) are known to be composite members, are primarily used in the lateral resistance systems of both braced and unbraced structures/components. Concrete-filled steel tube columns (CFSTCs) combine the advantages of ductility, generally associated with steel structures, with the stiffness of a concrete structural system. There are several applications in Japan and Europe where in CFSTs are also employed as bridge piers (Kitada 1998, Abdelkarim *et al*. 2015). Further, CFSTs were also utilized for retrofitting purposes to strengthen concrete columns in earthquake prone areas (Sakino and Sun 2000). Due to composite action, CFSTCs have notable advantages such as high compressive strength, stiffness, high tensile strength, ductility and enhanced flexural capacity. CFSTCs possess other advantages like (i) reduction of construction cost, (ii) no extra reinforcement is required since tube serves as longitudinal and lateral reinforcement for the concrete core, (iii) effective usage of steel, (iv) confining pressure to concrete, (v) reduced cross section, (vi) delay and often prevent local buckling of the steel member and (vii) economy. It was mentioned in the literature that the ultimate strength or failure load of CFSTCs depends on material properties and steel ratio (O'Shea and Bridge 2000, Schneider 1998, Sakino *et al*. 2004, Johansson and Gylltoft 2002, Han and Yao 2004, Han *et al*. 2005). Various cross sections of CFSTs such as circular, square and rectangular, etc. were employed for the investigations. Generally, only plain concrete is infilled to the hollow tubes. Some situations, where ductility and fire resistance are of paramount, fibers are to be added to concrete, in such cases the workability of the concrete should be ensured. Several investigations were carried out on CFSTs having various grades of concrete (Liu *et al*. 2003, Liu and Gho 2005, Lue *et al*. 2007, Yu *et al*. 2008, Uy 2001, Aslani *et al*. 2015). The axial load capacity of CFST columns with several grades such as 30, 60 and 100 MPa were examined depending on the effects of various steel tube thickness by Giakoumelis and Lam (2004). The experimental results indicated that the Eurocode 4, American Concrete Institute, and Australian Standards predict conservatively the axial load capacities of normal and high-strength CFSTCs. Many parametric studies were carried out on circular normal and high-strength CFSTCs by Ellobody *et al*. (2006). From the studies, it was found that the design strengths obtained by the ACI and the AS design codes are found to be conservative, but EC4 generally overestimates. Lam and Gardner (2008) carried out series of tests on the behavior of axially loaded square and circular CFST columns with concrete compressive strengths varying from 30 to 100 MPa. It was found that EC4 and Architectural Institute of Japan design codes yielded conservative and can be applied safely to normal strength CFSTCs. Xiong *et al*.

*Corresponding author, Assistant Professor,
E-mail: cigdem.karatas@yalova.edu.tr

ISSN: 1229-9367 (Print), 1598-6233 (Online)

(2017) carried out extensive investigations on CFSTs with high and ultrahigh strength concrete. A general observation is that it takes considerable amount of time and effort to carry out experiment. Further, numerical simulation requires accurate modeling to represent the realistic behavior of experimental findings. In the present scenario, several statistical models proposed and implemented by many researchers will be useful for adopt and to predict the experimental responses. The models include, artificial neural network, relevance vector machine, support vector machine, multivariate adaptive regression splines, Gaussian process regression, extreme learning machine, least-squares support vector machine (Yuvaraj *et al*. 2014, Parab *et al*. 2014, Shah *et al*. 2014, Dutta *et al*. 2017, Kaur and Kaur 2017, Erdem 2017, Engin *et al*. 2015).

Ultimate capacity prediction of axially loaded CFST short columns was provided by Guneyisi *et al*. (2016) using gene expression programming (GEP). Ren *et al*. (2019) investigated the application of the combined PSVM model (support vector machine (SVM) optimized by particle swarm optimization (PSO)) in the prediction of ultimate axial capacity of square CFST short columns. After careful study of all the models, it is noticed that each model has its own merits and limitations.

This paper employs multivariate adaptive regression splines (MARS) to develop a model to predict ultimate load capacity of CFSTCs. MARS is a statistical model which accounts the nonlinear behavior of the system for reliable and accurate prediction. Mansouri *et al*. (2016) predicted the strength of rotary brace damper by employing multiple linear regressions (MLR) and MARS methods. Lokuge *et al*. (2018) proposed a mix design methodology for fly ash based geopolymer concrete mix based on the concepts of MARS. Li and Yang (2018) assessed the tensile strain hardening capacity of fiber reinforced cementitious composites by using probabilistic based approach considering material heterogeneity. Tensile strain hardening was measured in terms performance indices which are obtained by using MARS. Cheng and Cao (2016) predicted the strength of concrete incorporated with rubber by using evolutionary MARS and also predicted shear strength of RC deep beams. Yuvaraj *et al*. (2013) used MARS model to predict the fracture characteristics of high strength and ultra-high strength concrete beams and found that a good agreement between predicted and experimental responses. In order to build a proper MARS model, one has to carefully focus on certain parameters such as (i) maximum number of basis function M_{max}, (ii) penalty parameter (smooth parameter) d and (iii) maximum interaction between variables mi. These parameters are found to be useful for generalization of the model as well as reduction of complexity of the model.

It can be noted that the application of MARS concepts in civil/structural engineering are found to be limited in the literature. So far, to knowledge of the author, while CFSTCs have merit in seismic applications, no guidance exists to help the engineer to predict ultimate load capacities using MARS with a reasonable degree of accuracy in the current technical literature. In this study, the experimental behaviors of axially loaded various circular CFSTCs are consolidated and developed an analytical model by using the concepts of MARS to predict ultimate axial load capacity of CFSTCs. The reliability of the developed new model has been validated with a data set comprising 150 experimental data results available in the literature.

2. Experimental investigations for CFSTCs with circular section

Several experimental investigations were reported in the literature on the performance of circular CFSTCs under axial compression loadings. From the wide literature review, it was observed the ultimate axial load capacity P_u is dependent on various factors such as (i) outer diameter of steel tube, D (ii) wall thickness of steel tube, t (iii) unconfined concrete strength, f_c (iv) Young's modulus of concrete, E_c (v) yield strength of steel, f_y (vi) Young's modulus of steel, E_s (vii) length of CFSTC, L (viii) confinement factor, ξ. Experimental data for stub/short CFSTCs were collected with a total of 150 CFSTCs from 22 different sources and will be used to develop and verify the MARS model.

Table 1 presents the geometrical parameters (namely, cross-section properties), material strength properties of concrete and steel and failure load of various circular CFSTCs with different confinement factors under axial load. The test data has a wide range of column parameters and the parameters for the test specimens are ranging from normal to high yield strength steels ($f_y = 186\sim853\ MPa$),

Table 1 Experimental test data for general details and ultimate load capacity of circular CFSTCs

Data Source	Test specimens	D (mm)	t (mm)	f_c (MPa)	E_c (MPa)	f_y (MPa)	E_s (MPa)	L (mm)	ξ	D/t	L/D	P_u (kN)
Gardener and Jacobson (Gardener and Jacobson 1967, Gardener 1968)	SPICIMEN8	120.8	4.06	34.40	27566	452	191536	241.3	1.962	30	2.0	1201
	SPICIMEN9	120.8	4.09	29.58	25562	452	191536	241.4	2.300	30	2.0	1201
	SPICIMEN10	120.8	4.09	25.92	23928	452	191536	241.4	2.625	30	2.0	1112
	SPICIMEN13	152.6	3.18	20.89	21482	415	203395	304.8	1.766	48	2.0	1201
	SPICIMEN14	152.6	3.15	23.10	22589	415	203395	304.8	1.581	48	2.0	1201
	SPICIMEN4	101.7	3.07	31.16	26236	605	207050	203.3	2.575	33	2.0	1068
	SPICIMEN3	101.7	3.07	34.13	27458	605	207050	203.3	2.351	33	2.0	1112
	SPICIMEN3a	169.3	2.62	36.54	28411	317	195811	305	0.563	65	1.8	1307

Table 1 Continued

Data Source	Test specimens	D (mm)	t (mm)	f_c (MPa)	E_c (MPa)	f_y (MPa)	E_s (MPa)	L (mm)	ξ	D/t	L/D	P_u (kN)
Tomii *et al*. (1977)	4HN	150	4.3	28.71	25183	280	209720	450	1.222	35	3.0	1203
	4HN	150	4.3	28.71	25183	280	209720	450	1.222	35	3.0	1225
	4HN	150	4.3	28.71	25183	280	209720	450	1.222	35	3.0	1200
	3HN	150	3.2	28.71	25183	287	190120	450	0.911	47	3.0	1040
	3HN	150	3.2	28.71	25183	287	190120	450	0.911	47	3.0	998
	3HN	150	3.2	28.71	25183	287	190120	450	0.911	47	3.0	980
	2HN	150	2	28.71	25183	336	211680	450	0.65	75	3.0	882
	2HN	150	2	28.71	25183	336	211680	450	0.65	75	3.0	882
	4MN	150	4.3	21.95	22020	280	209720	450	1.599	35	3.0	1065
	4MN	150	4.3	21.95	22020	280	209720	450	1.599	35	3.0	1087
	4MN	150	4.3	21.95	22020	280	209720	450	1.599	35	3.0	1096
	3MN	150	3.2	21.95	22020	287	190120	450	1.191	47	3.0	841
	3MN	150	3.2	21.95	22020	287	190120	450	1.191	47	3.0	840
	3MN	150	3.2	21.95	22020	287	190120	450	1.191	47	3.0	858
	2MN	150	2	21.95	22020	336	211680	450	0.85	75	3.0	773
	2MN	150	2	21.95	22020	336	211680	450	0.85	75	3.0	756
	4LN	150	4.3	18.03	19957	280	209720	450	1.946	35	3.0	963
	3LN	150	3.2	18.03	19957	287	190120	450	1.45	47	3.0	790
	3LN	150	3.2	18.03	19957	287	190120	450	1.45	47	3.0	790
	3LN	150	3.2	18.03	19957	287	190120	450	1.45	47	3.0	747
	2LN	150	2	18.03	19957	336	211680	450	1.035	75	3.0	656
	2LN	150	2	18.03	19957	336	211680	450	1.035	75	3.0	638
	2LN	150	2	18.03	19957	336	211680	450	1.035	75	3.0	672
Sakino and Hayashi (1991)	L-20-1	178	9	22.15	22120	283	200000	360	3.036	20	2.0	2042
	L-20-2	178	9	22.15	22120	283	200000	360	3.036	20	2.0	2102
	H-20-1	178	9	45.37	31658	283	200000	360	1.482	20	2.0	2667
	H-20-2	178	9	45.37	31658	283	200000	360	1.482	20	2.0	2677
	L-32-1	179	5.5	22.15	22120	248	200000	360	1.514	33	2.0	1467
	L-32-2	179	5.5	23.91	22982	248	200000	360	1.403	33	2.0	1530
	H-32-1	179	5.5	43.61	31038	248	200000	360	0.769	33	2.0	2040
	H-32-2	179	5.5	43.61	31038	248	200000	360	0.769	33	2.0	2030
	L-58-1	174	3	23.91	22982	266	200000	360	0.809	58	2.1	1135
	L-58-2	174	3	23.91	22982	266	200000	360	0.809	58	2.1	1135
	H-58-1	174	3	45.67	31762	266	200000	360	0.423	58	2.1	1608
	H-58-2	174	3	45.67	31762	266	200000	360	0.423	58	2.1	1677
O'Shea and Bridge (1994, 1998)	R12CF1	190	1.15	110.3	32405	202	193200	662	0.045	165	3.5	2991
	R12CF3	190	1.15	110.3	32405	202	193200	662	0.045	165	3.5	3137
	S10CS50A	190	0.86	41	17810	211	177000	659	0.094	221	3.5	1350
	S12CS50A	190	1.13	41	17810	186	178400	664.5	0.11	168	3.5	1377
	S16CS50B	190	1.52	48.3	21210	306	207400	664.5	0.208	125	3.5	1695
	S20CS50A	190	1.94	41	17810	256	204700	663.5	0.263	98	3.5	1678
	S30CS50B	165	2.82	48.3	21210	363	200600	580.5	0.541	59	3.5	1662
	S10CS80B	190	0.86	74.7	27576	211	177000	663.5	0.052	221	3.5	2451
	S12CS80A	190	1.13	80.2	28445	186	178400	662.5	0.056	168	3.5	2295
	S16CS80A	190	1.52	80.2	28445	306	207400	663.5	0.125	125	3.5	2602

Table 1 Continued

Data Source	Test specimens	D (mm)	t (mm)	f_c (MPa)	E_c (MPa)	f_y (MPa)	E_s (MPa)	L (mm)	ξ	D/t	L/D	P_u (kN)
	S20CS80B	190	1.94	74.7	27576	256	204700	663.5	0.144	98	3.5	2592
	S30CS80A	165	2.82	80.2	28445	363	200600	580.5	0.326	59	3.5	2295
Scneider (1998)	C1	140.8	3	28.18	25599	285	189475	602	0.92	47	4.3	790
	C2	141.4	6.5	23.81	23528	313	206011	602	2.797	22	4.3	1332
Tan *et al*. (1999)	A1-1	125	1	106	48389	232	200000	438	0.072	125	3.5	1275
	A1-2	125	1	106	48389	232	200000	438	0.072	125	3.5	1239
	A2-1	127	2	106	48389	258	200000	445	0.161	64	3.5	1491
	A2-2	127	2	106	48389	258	200000	445	0.161	64	3.5	1339
	A3-1	133	3.5	106	48389	352	200000	465	0.379	38	3.5	1995
	A3-2	133	3.5	106	48389	352	200000	465	0.379	38	3.5	1991
	A4-1	133	4.7	106	48389	352	200000	465	0.524	28	3.5	2273
	A4-2	133	4.7	106	48389	352	200000	465	0.524	28	3.5	2158
	C-1	133	4.7	92	45081	352	200000	465	0.604	28	3.5	1854
	C-2	133	4.7	92	45081	352	200000	465	0.604	28	3.5	1933
Yamamoto *et al*. (2000)	C10A-2A-3	101.8	3.03	23.2	22638	371	200000	305	2.088	34	3.0	628
	C20A-2A	216.4	6.61	24.3	23169	452	200000	650	2.499	33	3.0	3278
	C30A-2A	318.3	10.36	24.2	23121	335	200000	950	1.995	31	3.0	6319
	C20A-4A	216.4	6.61	46.8	32153	452	200000	650	1.298	33	3.0	4214
	C10A-4A-1	101.9	3.03	51.3	33663	371	200000	305	0.943	34	3.0	877
	C30A-4A	318.5	10.36	52.2	33957	334	200000	950	0.921	31	3.0	8289
Huang *et al*. (2002)	CU-040	200	5	27.15	24490	266	200000	600	1.058	40	3.0	1951
	CU-070	280	4	31.15	26232	273	200000	840	0.523	70	3.0	3025
	CU-150	300	2	27.23	24526	342	200000	900	0.342	150	3.0	2608
Han and Yao (2004)	scv2-1	200	3	49.5	37420	304	206500	600	0.386	67	3.0	2383
	scv2-2	200	3	49.5	37420	304	206500	600	0.386	67	3.0	2256
Giakomelis and Lam (2004)	C7	114.9	4.91	28.23	24972	365	200000	300.5	2.53	23	2.6	1020
	C9	115	5.02	48.6	32765	365	200000	300.5	1.506	23	2.6	1378
	C11	114.3	3.75	48.6	32765	343	200000	300	1.026	30	2.6	1033
	C12	114.3	3.85	25.71	23831	343	200000	300	1.997	30	2.6	761
	C4	114.6	3.99	83.6	42974	343	200000	300	0.637	29	2.6	1308
	C8	115	4.92	94.9	45786	365	200000	300	0.753	23	2.6	1787
	C14	114.5	3.84	88.9	44315	343	200000	300	0.575	30	2.6	1359
Sakino *et al*. (2004)	CC4-A-4-1	149	2.96	40.5	29911	308	200000	447	0.642	50	3.0	1064
	CC8-A-8	108	6.47	77	41242	853	200000	324	3.221	17	3.0	2667
	CC8-C-8	222	6.47	77	41242	843	200000	666	1.397	34	3.0	7304
	CC8-D-8	337	6.47	85.1	43357	823	200000	1011	0.788	52	3.0	13776
	CC4-D-4-1	450	2.96	41.1	30131	279	200000	1350	0.182	152	3.0	6870
	CC4-D-4-2	450	3	41	30131	279	200000	1350	0.182	152	3.0	6985
Han *et al*. (2005)	CA1-1	60	1.87	75.2	41540	282	201500	180	0.515	32	3.0	312
	CA1-2	60	1.87	75.2	41540	282	201500	180	0.515	32	3.0	320
	CA2-1	100	1.87	75.2	41540	282	201500	300	0.297	53	3.0	822
	CA2-2	100	1.87	75.2	41540	282	201500	300	0.297	53	3.0	845
	CA3-1	150	1.87	75.2	41540	282	201500	450	0.194	80	3.0	1701
	CA3-2	150	1.87	75.2	41540	282	201500	450	0.194	80	3.0	1670
	CA4-1	200	1.87	75.2	41540	282	201500	600	0.144	107	3.0	2783

Table 1 Continued

Data Source	Test specimens	D (mm)	t (mm)	f_c (MPa)	E_c (MPa)	f_y (MPa)	E_s (MPa)	L (mm)	ξ	D/t	L/D	P_u (kN)
	CA4-2	200	1.87	75.2	41540	282	201500	600	0.144	107	3.0	2824
	CA5-1	250	1.87	75.2	41540	282	201500	750	0.115	134	3.0	3950
	CA5-2	250	1.87	75.2	41540	282	201500	750	0.115	134	3.0	4102
	CB2-1	100	2	75.2	41540	404	207000	300	0.457	50	3.0	930
	CB2-2	100	2	75.2	41540	404	207000	300	0.457	50	3.0	920
	CB3-1	150	2	75.2	41540	404	207000	450	0.298	75	3.0	1870
	CB3-2	150	2	75.2	41540	404	207000	450	0.298	75	3.0	1743
	CB4-1	200	2	75.2	41540	404	207000	600	0.222	100	3.0	3020
	CB4-2	200	2	75.2	41540	404	207000	600	0.222	100	3.0	3011
	CB5-1	250	2	75.2	41540	404	207000	750	0.176	125	3.0	4442
	CB5-2	250	2	75.2	41540	404	207000	750	0.176	125	3.0	4550
	CC2-1	150	2	80	41540	404	207000	450	0.281	75	3.0	1980
	CC2-2	150	2	80	41540	404	207000	450	0.281	75	3.0	1910
	CC3-1	250	2	80	41540	404	207000	750	0.166	125	3.0	4720
	CC3-2	250	2	80	41540	404	207000	750	0.166	125	3.0	4800
Gupta *et al*. (2007)	D3M4C2	89.32	2.74	33	26999	360	200000	340	1.473	33	3.8	494
	D3M4F13	89.32	2.74	31.48	26370	360	200000	340	1.544	33	3.8	495
	D3M4F22	89.32	2.74	31.48	26370	360	200000	340	1.544	33	3.8	478
	D3M4F33	89.32	2.74	28.19	24954	360	200000	340	1.724	33	3.8	529
	D4M4C1	112.6	2.89	30.84	26101	360	200000	340	1.297	39	3.0	702
	D4M4F13	112.6	2.89	31.48	26370	360	200000	340	1.271	39	3.0	757
	D4M4F21	112.6	2.89	25.28	23631	360	200000	340	1.583	39	3.0	659
	D4M4F32	112.6	2.89	26.2	24057	360	200000	340	1.527	39	3.0	638
Yu *et al*. (2007)	SZ3S4A1	165	2.72	48	32563	350	213000	510	0.506	61	3.1	1750
	SZ3S6A1	165	2.73	67.2	38529	350	213000	510	0.363	60	3.1	2080
de Oliveira (2009)	C-30-3D	114.3	3.35	32.7	26876	287	206000	342.9	1.128	34	3.0	669
	C-60-3D	114.3	3.35	58.7	36009	287	206000	342.9	0.629	34	3.0	946
	C-80-3D	114.3	3.35	88.8	44290	287	206000	342.9	0.416	34	3.0	1133
	C-100-3D	114.3	3.35	105.5	48275	287	206000	342.9	0.350	34	3.0	1455
Lee *et al*. (2011)	049C36 30	360	6	31.5	26379	498	202000	1760	1.109	60	4.9	6888
Xiong *et al*. (2017)	C3	114.3	3.6	173.5	63000	403	213000	250	0.323	32	2.2	2422
	C4	114.3	3.6	173.5	63000	403	213000	250	0.323	32	2.2	2340
	C5	114.3	3.6	184.2	63000	403	213000	250	0.304	32	2.2	2497
	C6	114.3	3.6	184.2	63000	403	213000	250	0.304	32	2.2	2314
	C7	114.3	6.3	173.5	63000	428	209000	250	0.649	18	2.2	2610
	C8	114.3	6.3	173.5	63000	428	209000	250	0.649	18	2.2	2633
	C9	219.1	5	51.6	28000	377	205000	600	0.684	44	2.7	3118
	C10	219.1	5	185.1	66000	377	205000	600	0.199	44	2.7	7813
	C11	219.1	5	193.3	66000	377	205000	600	0.191	44	2.7	8527
	C12	219.1	10	51.6	28000	381	212000	600	1.489	22	2.7	4309
	C13	219.1	10	185	66000	381	212000	600	0.435	22	2.7	9085
	C14	219.1	10	193.3	66000	381	212000	600	0.416	22	2.7	9187
	C15	219.1	6.3	163	66000	300	202000	600	0.231	35	2.7	6915
	C16	219.1	6.3	175.4	59000	300	202000	600	0.215	35	2.7	7407

Table 1 Continued

Data Source	Test specimens	D (mm)	t (mm)	f_c (MPa)	E_c (MPa)	f_y (MPa)	E_s (MPa)	L (mm)	ξ	D/t	L/D	P_u (kN)
	C17	219.1	6.3	148.8	52000	300	202000	600	0.254	35	2.7	6838
	C18	219.1	6.3	174.5	52000	300	202000	600	0.216	35	2.7	7569
Guler *et al*. (2013, 2014)	CF3-1	76.19	2.99	145	56595	278	200000	300	0.341	25	3.9	795
	CF3.3-1	76.18	3.31	145	56595	305	200000	300	0.419	23	3.9	847
	C4NG-1	114.2	4.02	115	50402	306	200000	400	0.418	28	3.5	1428
	C6NG-1	114.3	5.98	115	50402	314	200000	400	0.675	19	3.5	1833
Han *et al*. (2014)	c0	160	3.83	51	33900	409	200000	480	0.827	42	3.0	2023

from normal concrete strength to ultra-high strength concrete with an unconfined concrete strength ($f_c = 18\sim193\ MPa$), outer diameter of circular sections ($D = 60\sim450\ mm$), the ratio of the outer diameter to the thickness ($D/t = 17\sim221$) and the ratio of the length to outer diameter ($L/D = 1.8 - 4.9$), respectively. As can be observed in Table 1, these parameters cover sufficiently wide practical ranges.

3. Multivariate adaptive regression splines (MARS)

MARS is an advanced statistical technique first proposed by Friedman (Friedman and Silverman 1989, Friedman 1991). MARS concepts can be employed for development of models by training the data. Various relationships can be established among the input and output data. It has been found that using the MARS concepts, the relations can be established easily among the dependent variables. Basically, this technique identifies the critical variables that form input and output. MARS critically examines the relationship between input variables and the response of output variables. Based on the response, the interactions and conditional relationships can be identified between the predictor variables. MARS attempts to establish the unknown functional form by using multilinear piecewise regression splines. The nonlinear relationship between some input variables and output can be treated as piecewise linear so that all the dependent input and output variables can be treated in similar manner. MARS discards certain data which is over-fitting in nature and also inconsistencies in the data. MARS can also identify the interdependent variables. Separate regression lines can be formed through the concept of divide and conquers strategy.

MARS is widely recognized and accepted by research and practitioners community due to many reasons such as (i) MARS establishes the nonlinear relationship among variables with no model assumptions (ii) it captures the relative importance of independent variables to the dependent variable if there are several independent variables (iii) the training data set in MARS is relatively faster than other statistical models and (iv) interpretations can be drawn easily. The following are the important steps to develop a MARS based model:

- Dividing the training data into many splines on an equivalent interval basis.
- The data can further be divided into many subgroups and forms several knots, which can be located between various input variables or various intervals within the same input variable, to separate the subgroups.
- To represent the data, in each subgroup, the model approximates a regression function using smoothing splines, which is known as a basis function (BF).
- Piecewise polynomials have pieces which connect together and the intersection points are called knots.
- Between any two knots, the model can characterize the data between any two knots either globally or by using linear regression.
- Between any two knots, the BF is unique and is shifted to another BF at each knot.
- In order to make the model output continuous, the two BFs in two adjacent domains of data intersect at the knot.
- Finally, MARS generates a mixed regression line to fit the data from various subgroups to subgroups and from splines to splines.
- To avoid over fitting and over regressing, the shortest distance between two neighboring knots can be pre-determined to prevent too few data in a subgroup.

MARS function is expressed by the equation as follows (Friedman 1988, 1991)

$$y = \hat{f}(x) = a_0 + \sum_{m=1}^{M} a_m B_m^{(q)}(x) \quad (1)$$

where, $a_0 =$ coefficient of the constant BF, $m =$ number of non-constant BFs, $\{a_m\}_1^M =$ vector of coefficients of the non-constant BFs $(m = 1, 2, \dots, M)$, $B_m^{(q)} =$ BFs that are selected for inclusion in the model of q^{th}order.

$$B_m^{(q)}(x) = \prod_{k-1}^{k_m} \left[s_{km} \cdot (x_{v(k,m)} - t_{km}) \right]_+^q \quad (2)$$

where $B_m^{(q)}(x) =$ vector of non-constant (truncated) BFs (see Fig. 1), $m =$ number of non-constant functions $(1,2, \dots, M)$, $q =$ the power to which the spline is raised to control the degree of smoothness of the resultant function estimate if, the power is $+=$ only positive results of the

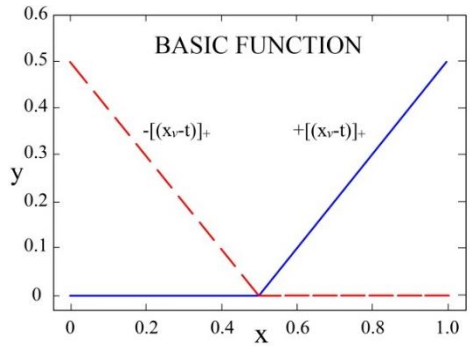

Fig. 1 Typical BF

right-hand side of the equation will be considered, otherwise, the functions evaluate to 0, $s_{km} =$ indicates the (left/right) sense of truncation, which has only 2 values (± 1). For s_{km} equal to $+1$, the BF has a value $x - t$ if $x > t$ and 0 if $x \leq t$. If it is -1, the BF has a value $t - x$ when $x < t$, while 0 if $x \geq t$; $x_{v(k,m)} =$ value of the predictor, $v(k,m) =$ label of the predictor ($1 \leq v(k,m) \leq n$), $n =$ number of predictors, $t_{km} =$ "knot" location on the corresponding predictor region, or value that defines an inflection point, $K =$ maximum level or order of interaction, or the number of factors, in the m^{th} BF ($1,2, \dots, K_m$).

BFs contain set of functions required to represent the data of one or more variables. MARS parameters will be evaluated by using the penalized least squares of the form as given below in Eq. (3)

$$P(x) = \min \sum \left(y_i - \hat{f}(x_i)\right)^2 + \lambda \int f^n(x_i) dx_i \qquad (3)$$

The first term in Eq. (3), is the residual sum of squares and the other term, is the roughness penalty term, which is weighted by a smoothing constant λ. The penalty term is more when the integrated second derivative of the regression function $f''(x)$ is large, ie $f(x)$ is 'rough' (with rapidly changing slope). At one extreme, when the λ is set to zero, the objective function simply interpolates the data. For the case of other extreme, if λ is very large, then the objective function will be selected so that its second derivative is zero everywhere, indicating a globally linear least squares fit to the data (Fox 2002). Knots are chosen in an iterative forward stepwise procedure during the development of MARS model. One of the most useful applications of variable nesting in MARS is in focussing i^{th} missing values among the independent variables. MARS generates two BFs for any variable with missing data, one BF for the presence of missing values and another BF for the absence (Francis 2001).

It is to be noted that MARS does not account interactions with missing value indicators to be genuine interactions. There is possibility that if additive model is generated using MARS, it may still contain interactions related to missing value indicators. After over-fitting the model with many BFs, a snubbing procedure is carried out where in unproductive BFs will be removed. Even, a predictor variable will be dropped from the model if all corresponding BFs are not contribute meaningfully to predictive performance.

The models developed through this process are then evaluated using the generalized cross-validation (GCV), and the model with the best predictive fit is finally selected. The GCV can be calculated by using Eq. (4).

$$GCV(M) = \frac{\frac{1}{N}\sum_{i=1}^{N}\left[y_i - \overset{M}{\wedge} f(x_i)\right]^2}{\left[1 - \frac{C(M)}{N}\right]^2} \qquad (4)$$

In Eq. (4), the numerator denotes lack-of-fit on the training data and the denominator considers the penalty for increasing model complexity $C(M)$, $N =$ number of observations, $C(M) =$ cost penalty measures of a model, $M =$BFs, $F_m(x_i) =$ basis function model. Towards best fit of the model, MARS minimizes $GCV(M)$.

Friedman and Silverman (1989) suggested that by using Eq. (3) as a lack-of-fit criterion, proposed Eq. (5) to account for additional BF parameters. Typical complexity function can be expressed as

$$\tilde{C}(M) = C(M) + d.M \qquad (5)$$

where $C(M) =$ number of parameters being fitted, $M =$ number of non-constant BFs in the model BF parameters, $d =$ cost for each BF optimization and is a smoothing parameter of the procedure, Eq. (1) can be re-written in the following form

$$\hat{f}(x) = a_0 + \sum_{K_m=1} f_i(x_i) + \sum_{K_m=2} f_{ij}(x_i, x_j) + \sum_{K_m=3} (x_i, x_j, x_k) + \cdots \qquad (6)$$

This is known as ANOVA decomposition of the MARS model. The first term is a single variable corresponding to all BFs. The second term comprising of all BFs that involve exactly two variables and their interactions if any. Similarly, the third term signifies three variables and their interactions if any. More information about the model and the model building process can be found in Friedman (1991).

4. Mars based analysis and development of model

To predict the ultimate capacity of CFSTC, a model was developed by utilizing the concepts of MARS in MATLAB environment. From Table 1, it can be noticed that input vector has different quantitative limits and normalization of the data is required before processing the data. Eq. (7) is used for the linear normalization of the data, with the data ranging from 0 to 1.

$$x_i^n = \frac{x_i^a - x_i^{min}}{x_i^{max} - x_i^{min}} \qquad (7)$$

where x_i^a and x_i^n are the i^{th} components of the input vector before and after normalization, respectively, and x_i^{max} and x_i^{min} are the maximum and minimum values of

all the components of the input vector before the normalization. The MARS equation for the prediction of ultimate load capacity of CFSTCs is given by Eq. (8). Initially, about 25 BFs have been employed to build the model and the final model was with 20BFs (see in Table 2). The highest degree of interaction was set to 2. The Eq. (1) will become as below

$$y = P_{max} = 0.359 + \sum_{m=1}^{20} a_m B_m^1(x) \tag{8}$$

In the Table 3, the ANOVA decomposition is presented in row wise for each ANOVA function. The columns contain the corresponding quantities for corresponding ones. The first column is the function number. The second is the standard deviation (STD) of the function, which is very important and is same as a standard regression coefficient in a linear model. The third column contains the GCV score corresponding to BFs and combination of BFs. This score has very significant value to judge whether corresponding ANOVA function contribution is meaningful or not. The fourth column is the number of BFs consisting the ANOVA and the last column of Table 3 presents the corresponding predictor variables associated with the ANOVA function.

The value of coefficient of correlation (R) is determined by using Eq. (9)

Table 2 Final BFs to build a model for the prediction of ultimate capacity of CFSTC

BF $B_m^1(x)$	Equation	Coefficient (a_m)
$B_1(x)$	max $(0,\ f_c - L/D)$	1.212
$B_2(x)$	max $(0,\ L/D - f_c)$	-0.165
$B_3(x)$	max $(0, L - D/t)$	-0.321
$B_4(x)$	max $(0, D/t - L)$	-0.632
$B_5(x)$	max $(0,\ f_c * \xi)$	2.654
$B_6(x)$	$B_3(x) *$ max $(0,\ L/D - 4.9)$	-2.054
$B_7(x)$	$B_3(x) *$ max$(0, 221 - D/t)$	3.165
$B_8(x)$	$B_5(x) *$ max $(0,\ L/D)$	4.654
$B_9(x)$	$B_3(x) *$ max $(0,\ f_c * \xi)$	1.876
$B_{10}(x)$	$B_4(x) *$ max $(0, f_y * \xi)$	0.721
$B_{11}(x)$	$B_3(x) *$ max $(0, 193 - f_c)$	0.312
$B_{12}(x)$	$B_4(x) *$ max $(0,\ f_y - 853)$	-2.321
$B_{13}(x)$	$B_3(x) *$ max $(0,\ E_c - 66000)$	0.08
$B_{14}(x)$	max $(193 - f_c) *$ max $(0, f_y - 853)$	4.167
$B_{15}(x)$	max $(0,\ f_c - 193)$	0.127
$B_{16}(x)$	$B_1(x) *$ max $(0, E_s - 213000)$	3.156
$B_{17}(x)$	$B_2(x) *$ max $(0, 853 - f_y)$	-1.765
$B_{18}(x)$	$B_3(x) *$ max $(0, 213000 - E_s)$	-0.543
$B_{19}(x)$	$B_2(x) * (0, \xi * E_s - 213000)$	2.654
$B_{20}(x)$	$B_2(x) *$ max $(0, 213000 - \xi * E_s)$	-0.245

$$R = \frac{\sum_{i=1}^{n}(E_{ai} - \overline{E}_a)(E_{pi} - \overline{E}_p)}{\sqrt{\sum_{i=1}^{n}(E_{ai} - \overline{E}_a)}\sqrt{\sum_{i=1}^{n}(E_{pi} - \overline{E}_p)}} \tag{9}$$

where E_{ai} and E_{pi} are the actual and the predicted values, respectively, and are mean of actual and predicted E values corresponding to n patterns.

The key features of the developed model are tabulated in Table 4. On successful development of MARS model with 105 dataset, the model is verified with remaining 40 dataset. Table 5 shows the results of ultimate load capacity of CFSTCs predicted with MARS modeling and experimentally, respectively.

Since, the output vector obtained from the MARS model is a normalized data; it has been reverted to its actual value

Table 3 ANOVA decomposition –ultimate axial load capacity (P_u)

Func.	STD	GCV	#basis	Variable(s)
1	0.127	0.102	2	f_c, L, D
2	0.329	0.31	2	f_c, L, D
3	0.421	0.483	2	L, D, t
4	0.273	0.201	5	L, D, t
5	0.106	0.028	2	f_c, ξ
6	0.107	0.027	1	L, D
7	0.144	0.07	4	D, t
8	0.231	0.12	1	L, D
9	0.124	0.032	2	f_c
10	0.201	0.02	3	f_y
11	0.214	0.134	1	f_c, ξ
12	0.112	0.034	2	f_y
13	0.321	0.102	1	E_c
14	0.102	0.06	2	f_c, f_y
15	0.284	0.102	2	f_c
16	0.301	0.07	1	E_s
17	0.261	0.112	3	f_y
18	0.318	0.142	2	E_s
19	0.156	0.08	2	ξ, E_s
20	0.286	0.01	1	ξ, E_s

Table 4 The key features of the developed model

User defined max. no. of BFs		25
Interactions ratio allowed		2
Final number of BFs		20
Mean square error	Training	$6.34E-05$
	Testing	$8.65E-04$
Root mean square error		0.0332
Generalized cross validation		$3.21E-04$
Coefficient of correlation (R)	Training	0.993
	Testing	0.995

Table 5 Comparison of ultimate load capacity values between experimental and predicted with MARS modeling

$f_c\ (MPa)$	$f_y\ (MPa)$	D/t	L/D	ξ	$P_u^E(kN)$	$P_u^{MARS}(kN)$	P_u^{MARS}/P_u^E
34.40	452	30	2.0	1.962	1201	1125	0,94
31.16	605	33	2.0	2.575	1068	930	0,87
36.54	317	65	1.8	0.563	1307	1265	0,97
28.71	287	47	3.0	0.911	998	980	0,98
28.71	336	75	3.0	0.65	882	802	0,91
21.95	336	75	3.0	0.85	773	790	1,02
18.03	336	75	3.0	1.035	656	660	1,01
22.15	283	20	2.0	3.036	2042	1978	0,97
45.37	283	20	2.0	1.482	2667	2489	0,93
22.15	248	33	2.0	1.514	1467	1402	0,96
43.16	248	33	2.0	0.769	2040	1965	0,96
23.91	266	58	2.1	0.809	1135	1098	0,97
45.67	266	58	2.1	0.423	1677	1689	1,01
110.3	202	165	3.5	0.045	3137	2876	0,92
80.2	306	125	3.5	0.125	2602	2453	0,94
28.18	285	47	4.3	0.92	790	710	0,90
106	258	64	3.5	0.161	1339	1280	0,96
106	352	28	3.5	0.524	2158	2087	0,97
96	358	24	3.5	0.709	1518	1432	0,94
23.2	371	34	3.0	2.088	628	643	1,02
46.8	452	33	3.0	1.298	4214	3798	0,90
52.2	334	31	3.0	0.921	8289	7654	0,92
31.15	273	70	3.0	0.523	3025	2865	0,95
49.5	304	67	3.0	0.386	2256	2076	0,92
83.6	343	29	2.6	0.637	1308	1207	0,92
88.9	343	30	2.6	0.575	1359	1287	0,95
77	853	17	3.0	3.221	2667	2543	0,95
77	843	34	3.0	1.397	7304	7021	0,96
85.1	823	52	3.0	0.788	13776	12765	0,93
41	279	152	3.0	0.1582	6985	6340	0,91
75.2	282	32	3.0	0.515	320	352	1,10
75.2	282	53	3.0	0.297	845	893	1,06
75.2	282	107	3.0	0.144	2783	2521	0,91
75.5	282	134	3.0	0.115	3950	3652	0,92
75.2	404	50	3.0	0.457	920	821	0,89
75.2	404	125	3.0	0.176	4442	4129	0,93
31.48	360	33	3.8	1.544	478	432	0,90
26.2	360	39	3.0	1.527	638	610	0,96
185.1	377	44	2.7	0.199	7813	7231	0,93
148.8	300	35	2.7	0.254	6838	6234	0,91

by using Eq. (10).

$$x_i^a = x_i^n\left(x_i^{max} - x_i^{min}\right) + x_i^{min} \tag{10}$$

where x_i^n is the normalized result obtained after the test corresponding to ith component. x_i^a is the actual result obtained corresponding to ith component, and x_i^{max} and x_i^{min} are the maximum and minimum values of input vector before the normalization.

5. Results of MARS model

From Table 5, it can be observed that the predicted ultimate axial load capacity values of P_u in MARS modeling are in very good agreement with the corresponding experimental data values. Fig. 2 shows the comparison ultimate axial load capacity values between experimental (P_u^E) and predicted with MARS modeling (P_u^{MARS}), respectively.

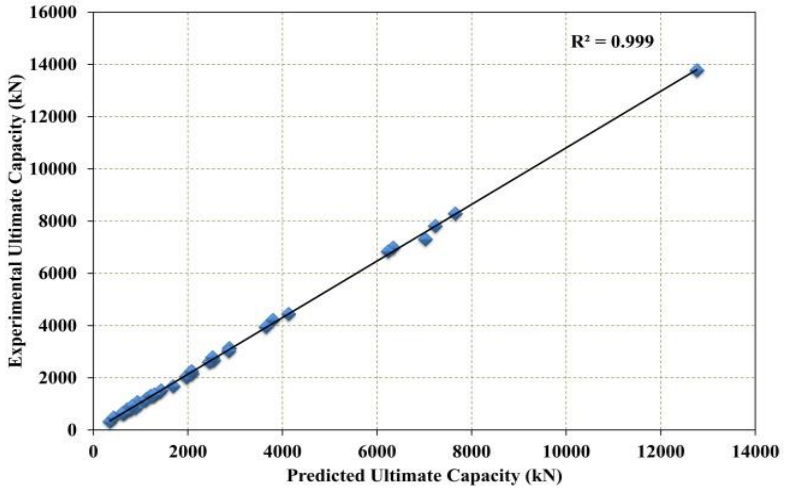

Fig. 2 Predicted vs experimental ultimate axial load capacity (P_u)

Close agreement between Mars modeling results and the corresponding experimental findings are observed for the developed model. The difference between the predicted and the corresponding experimental values is found to be less than 10%, hence the developed MARS model is robust and reliable.

6. Conclusions

In the present study, by employing MARS modeling concepts, an advanced statistical model has been developed to predict the ultimate load capacity of CFSTC member under axial loading. The existing experimental data on CFSTCs considering variation in geometrical and mechanical properties has been collected and consolidated for the development of model. Based on the experimental findings, MARS model established a relationship between a set of predicators and dependent variables. MARS is based on a divide and conquers strategy partitioning the training data sets into separate regions; each gets its own regression line. Key input variables have been identified for the prediction of ultimate load capacity of CFSTCs. MARS model has been developed by using MATLAB software for training and prediction of the failure load. Model has been developed by training about 70% of the mixed data (about 105 data sets) and the remaining data sets (about 45) have been used for validation of the developed model. It is observed that the predicted value of ultimate load capacity is in close agreement with those of the experimental values. The predicted ultimate load capacity is comparable with that of experimental value and the percentage difference between the predicted value and the corresponding experimental value is found to be less than 10%. The ratio of predicted and the corresponding experimental ultimate load P_u^{MARS}/P_u^E was found to vary in between 0.87 and 1.10. The model could serve as an alternative to experimental studies and hence the predicted ultimate load can be used for the design of CFSTC members.

References

Abdelkarim, O.I., Gheni, A., Anumolu, S., Wang, S. and ElGawady, M. (2015), "Hollow-core FRP-concrete-steel bridge columns under extreme loading", Report No. cmr15-008; Missouri Department of Transportation Research, Development and Technology, Missouri University of Science and Technology, MO, USA.

Aslani, F., Uy, B. and Tao, Z. and Mashiri, F. (2015), "Behaviour and design composite columns incorporating compact high-strength steel plates", *J. Constr. Steel Res.*, **107**, 94-110. https://doi.org/10.1016/j.jcsr.2015.01.005

Cheng, M.Y. and Cao, M.T. (2016), "Estimating strength of rubberized concrete using volutionary multivariate adaptive regression splines", *J. Civ. Eng. Manag.*, **22**(5), 711-720. https://doi.org/10.3846/13923730.2014.897989

de Oliveira, W.L.A., de Nardin, S., de Cresce El Debs, A.L.H. and El Debs, M.K. (2009), "Influence of concrete strength and length/diameter on the axial capacity of CFT columns", *J. Constr. Steel Res.*, **65**(12), 2103-2110. https://doi.org/10.1016/j.jcsr.2009.07.004

Dutta, S., Murthy, A.R., Kim, D. and Samui, P. (2017), "Prediction of compressive strength of self-compacting concrete using intelligent computational modelling", *CMC: Computers, Materials & Continua*, **53**(2), 157-174. https://doi.org/10.3970/cmc.2017.053.167

Ellobody, E., Young, B. and Lam, D. (2006), "Behavior of normal and high strength concrete-filled compact steel tube circular stub columns", *J. Constr. Steel Res.*, **62**(7), 706-715. https://doi.org/10.1016/j.jcsr.2005.11.002

Engin, S., Ozturk, O. and Okay, F. (2015), "Estimation of ultimate torque capacity of the SFRC beams using ANN", *Struct. Eng. Mech., Int. J.*, **53**(5), 939-956. https://doi.org/10.12989/sem.2015.53.5.939

Erdem, H. (2017), "Predicting the moment capacity of RC slabs with insulation materials exposed to fire by ANN", *Struct. Eng. Mech., Int. J.*, **64**(3), 339-346. http://dx.doi.org/10.12989/sem.2017.64.3.339

Fox, J. (2002), "Nonparametric Regression. Appendix to An R and S-PLUS Companion to Applied Regression", Salford Systems, Inc., "MARSTM User Guide".

Francis, L.A. (2001), "Neural Networks Demystified", *Casualty Actuarial Society Forum*, pp. 253-320.

Friedman, J.H. (1988), "Fitting Functions to Noisy Data in High Dimensions", Technical Report No. LCS101; Department of

Statistics, School of Humanities & Sciences, Standford University, Standford, CA, USA.
Friedman, J.H. (1991), "Multivariate adaptive regression splines", *The Annals of Statistics*, **19**(1), 1-67.
Friedman, J.H. and Silverman, B.W. (1989), "Flexible parsimonious smoothing and additive modelling". *Technometrics*, **31**, 3-39. https://doi.org/10.1080/00401706.1989.10488470
Gardener, N.J. (1968), "Use of spiral welded steel tubes in pipe columns", *J. Am. Concrete Inst. (ACI)*, **65**(11), 937-942.
Gardener, N.J. and Jacobson, R. (1967), "Structural behavior of concrete filled steel tubes", *J. Am. Concrete Inst. (ACI)*, **64**(7), 404-413.
Giakoumelis, G. and Lam, D. (2004), "Axial capacity of circular concrete-filled tube columns", *J. Constr. Steel Res.*, **60**(7), 1049-1068. https://doi.org/10.1016/j.jcsr.2003.10.001
Guler, S., Copur, A. and Aydogan, M. (2013), "Axial capacity and ductility of circular UHPC-filled steel tube columns", *Mag. Concrete Res.*, **65**(15), 898-905. https://doi.org/10.1680/macr.12.00211
Guler, S., Copur, A. and Aydogan, M. (2014), "A comparative study on square and circular high strength concrete-filled steel tube columns", *Adv steel Constr.*, **10**(2), 234-247. https://doi.org/10.18057/IJASC.2014.10.2.7
Guneyisi, E.M., Gultekin, A. and Mermerdas, K. (2016), "Ultimate capacity prediction of axially loaded CFST short columns", *Int. J. Steel Struct.*, **16**(1), 99-114. https://doi.org/10.1007/s13296-016-3009-9
Gupta, P.K., Sarda, S.M. and Kumar, M.S. (2007), "Experimental and computational study of concrete filled steel tubular columns under axial loads", *J. Constr. Steel Res.*, **63**(2), 182-193. https://doi.org/10.1016/j.jcsr.2006.04.004
Han, L.H. and Yao, G.H. (2004), "Experimental behaviour of thin-walled hollow structural steel (HSS) columns filled with self-consolidating concrete (SCC)", *Thin-Wall. Struct.*, **42**(9), 1357-1377. https://doi.org/10.1016/j.tws.2004.03.016
Han, L.H., Yao, G.H. and Zhao, X.L. (2005), "Tests and calculations for hollow structural steel (HSS) stub columns filled with self-consolidating concrete (SCC)", *J. Constr. Steel Res.*, **61**(9), 1241-1269. https://doi.org/10.1016/j.jcsr.2005.01.004
Han, L.H., Hou, C.C. and Wang, Q.L. (2014), "Behavior of circular CFST stub columns under sustained load and chloride corrosion", *J. Constr. Steel Res.*, **103**, 23-36. https://doi.org/10.1016/j.jcsr.2014.07.021
Huang, C.S., Yeh, Y.K., Liu, G.Y., Hu, H.T., Tsai, K.C., Weng, Y.T., Wang, S.H. and Wu, M.H. (2002), "Axial load behavior of stiffened concrete-filled steel columns", *J. Struct. Eng.*, ASCE, **128**(9), 1222-1230. https://doi.org/10.1061/(ASCE)0733-9445(2002)128:9(1222)
Johansson, M. and Gylltoft, K. (2002), "Mechanical behavior of circular steel–concrete composite stub columns", *J. Struct. Eng.*, ASCE, **128**(8), 1073-1081. https://doi.org/10.1061/(ASCE)0733-9445(2002)128:8(1073)
Kaur, J. and Kaur, K. (2017), "A fuzzy approach for an IoT-based automated employee performance appraisal", *CMC: Computers, Materials & Continua*, **53**(1), 23-36.
Kitada, T. (1998), "Ultimate strength and ductility of state-of-the-art concrete-filled steel bridge piers in Japan", *Eng. Struct.*, **20**(4-6), 347-354. https://doi.org/10.1016/S0141-0296(97)00026-6
Lam, D. and Gardner, L. (2008), "Structural design of stainless steel concrete filled columns", *J. Constr. Steel Res.*, **64**(11), 1275-1282. https://doi.org/10.1016/j.jcsr.2008.04.012
Lee, S.H., Uy, B., Kim, S.H., Choi, Y.H. and Choi, S.M. (2011), "Behavior of highstrength circular concrete-filled steel tubular (CFST) column under eccentric loading", *J. Constr. Steel Res.*, **67**, 1-13. https://doi.org/10.1016/j.jcsr.2010.07.003
Li, J. and Yang, E.H. (2018), "Probabilistic-based assessment for tensile strain-hardening potential of fiber-reinforced cementitious composites", *Cement Concrete Compos.*, **91**, 108-117. https://doi.org/10.1016/j.cemconcomp.2018.05.003
Liu, D.L. and Gho, W.M. (2005), "Axial load behaviour of high-strength rectangular concrete filled steel tubular stub columns", *Thin Wall Struct.*, **43**(8), 1131-1142. https://doi.org/10.1016/j.tws.2005.03.007
Liu, D.L., Gho, W.M. and Yuan, J. (2003), "Ultimate capacity of high-strength rectangular concrete-filled steel hollow section stub columns", *J Constr Steel Res.*, **59** (12), 1499-1515. https://doi.org/10.1016/S0143-974X(03)00106-8
Lokuge, W., Wilson, A., Gunasekara, C., Law, D.W. and Setunge, S. (2018), "Design of fly ash geopolymer concrete mix proportions using Multivariate Adaptive Regression Spline model", *Constr. Build. Mater.*, **166**(30), 472-481. https://doi.org/10.1016/j.conbuildmat.2018.01.175
Lue, D.M., Liu, J.L. and Yen, T. (2007), "Experimental study on rectangular CFST columns with high-strength concrete", *J. Constr. Steel Res.*, **63**(1), 37-44. https://doi.org10.1016/j.jcsr.2006.03.007
Mansouri, I., Safa, M., Ibrahim, Z., Kisi, O., Tahir, M.M., Baharom, S.B. and Azimi, M. (2016), "Strength prediction of rotary brace damper using MLR and MARS", *Struct. Eng. Mech., Int. J.*, **60**(3), 471-488. https://doi.org/10.12989/sem.2016.60.3.471
O'Shea, M.D. and Bridge, R.Q. (1994), "Tests on thin-walled concrete-filled steel tubes", *Proceedings of the 12th International Specialty Conference on Cold-Formed Steel Strucures*, St. Louis, MO, USA, October, pp. 399-419.
O'Shea, M.D. and Bridge, R.Q. (1998), "Tests on circular thin-walled steel tubes filled with medium and high strength concrete", *Austral. Civil Eng. Transact.*, **40**, 15-27.
O'Shea, M.D. and Bridge, R.Q. (2000), "Design of circular thin-walled concrete filled steel tubes", *J. Struct. Eng.*, ASCE, **126**(11), 1295-1303. https://doi.org/10.1061/(ASCE)0733-9445(2000)126:11(1295)
Parab, S., Srivastava, S., Samui, P. and Murthy, A.R. (2014), "Prediction of fracture parameters of high strength and ultra high strength concrete beams using gaussian process regression and least squares support vector machine", *CMES-Comp. Model. Eng.*, **101**(2), 139-158. https://doi.org/10.3970/cmes.2014.101.139
Ren, Q., Li, M., Zhang, M., Shen, Y. and Si, W. (2019), "Prediction of ultimate axial capacity of square concrete-filled steel tubular short columns using a hybrid intelligent algorithm", *Appl. Sci.*, **9**(14), 2802. https://doi.org/10.3390/app9142802
Sakino, K. and Hayashi, H. (1991), "Behavior of concrete filled steel tubular stub columns under concentric loading", *Proceedings of the 3rd International Conference on Steel Concrete Composite Structures*, Fukuoka, Japan, September, pp. 25-30.
Sakino, K. and Sun, Y. (2000), "Steel jacketing for improvement of column strength and ductility", *Proceedings of the 12th World Conference on Earthquake Engineering*, New Zealand.
Sakino, K., Nakahara, H., Morino, S. amd Nishiyama, I. (2004), "Behavior of centrally loaded concrete-filled steel-tube short columns" *J. Struct. Eng.*, **130**(2), 180-188. https://doi.org/10.1061/(ASCE)0733-9445(2004)130:2(180)
Schneider, S.P. (1998), "Axially loaded concrete-filled steel tubes", *J. Struct. Eng.*, ASCE, **124**(10), 1125-1138. https://doi.org/10.1061/(ASCE)0733-9445(1998)124:10(1125)
Shah, V.S., Shah, H.R., Samui, P. and Murthy, A.R. (2014), "Prediction of fracture parameters of high strength and ultra-high strength concrete beams using minimax probability machine

regression and extreme learning machine", *CMC: Computers, Materials & Continua*, **44** (2), 73-84. https://doi.org/10.3970/cmc.2014.044.073

Tan, K.F., Pu, X.C. and Cai, S.H. (1999), "Study on mechanical properties of extra strength concrete encased in steel tubes", *J. Build. Struct.*, **20**(1), 10-15. [In Chinese]

Tomii, M., Yoshimura, K. and Morishita, Y. (1977), "Experimental studies on concrete filled steel tubular stub columns under concentric loading", *Proceedings of the International Colloquium on Stability of Structures Under Static and Dynamic Loads*", Washington DC, USA, May, pp. 718-741.

Uy, B. (2001), Strength of short concrete filled high strength steel box columns", *J. Constr. Steel Res*., **57**(2), 113-134. https://doi.org/10.1016/S0143-974X(00)00014-6

Xiong, M.X., Xiong, D.X. and Liew, J.Y.R. (2017), "Axial performance of short concrete filled steel tubes with high- and ultra-high- strength materials", *Eng. Struct.*, **136**, 494-510. https://doi.org/10.1016/j.engstruct.2017.01.037

Yamamoto, T., Kawaguchi, J. and Morino, S. (2000), "Experimental study of scale effects on the compressive behavior of short concrete-filled steel tube columns", *Proceedings of the United Engineering Foundation Conference on Composite Construction in Steel and Concrete IV (AICE)*, Banff, Canada, June, pp. 879-891.

Yu, Z.W., Ding, F.X. and Cai, C.S. (2007), "Experimental behavior of circular concretefilled steel tube stub columns", *J. Constr. Steel Res.*, **63**, 165-174. https://doi.org/10.1016/j.jcsr.2006.03.009

Yu, Q., Tao, Z., Wu, Y.X. (2008), "Experimental behaviour of high performance concrete filled steel tubular columns", *Thin-Wall. Struct.*, **46**(4), 362-370. https://doi.org/10.1016/j.tws.2007.10.001

Yuvaraj, P., Murthy, A.R., Iyer, N.R., Samui, P. and Sekar, S.K. (2013), "Multivariate adaptive regression splines model to predict fracture characteristics of high strength and ultra high strength concrete beams", *CMC: Computers, Materials & Continua*, **36**(1), 73-97. https://doi.org/10.3970/cmc.2013.036.073

Yuvaraj, P., Murthy, A.R., Iyer, N.R., Samui, P. and Sekar, S.K. (2014), "Prediction of fracture characteristics of high strength and ultra high strength concrete beams based on relevance vector machine", *Int. J. Damage Mech.*, **23**(7), 979-1004. https://doi.org/10.1177/1056789514520796

CC